High-Pressure Phase Behavior of Carbon Dioxide with Ionic Liquids: 1-Alkyl-3-methylimidazolium Trifluoromethanesulfonate

Eun-Kyoung Shin and Byung-Chul Lee*

Department of Chemical Engineering and Nano-Bio Technology, Hannam University, 461-6 Jeonmin-dong, Yuseong-gu, Daejeon 305-811, South Korea

Solubility data of carbon dioxide (CO_2) in the ionic liquids 1-alkyl-3-methylimidazolium trifluoromethanesulfonate ([$C_n$mim][TfO]; $n = 2, 4, 6, 8$) are presented at pressures up to about 40 MPa and at temperatures between (303.85 and 344.55) K. The equilibrium pressure increased very steeply at high CO_2 concentrations. The solubility of CO_2 in the ionic liquids decreased with an increase in temperature. The CO_2 solubility increased with the increase in the alkyl chain length on the cation of the ionic liquids. The phase equilibrium data for the CO_2 + ionic liquid systems have been correlated using the Peng−Robinson equation of state.

Introduction

Ionic liquids are a class of organic salts that are liquid at or near room temperature. They are generally composed of a large asymmetric organic cation and either an organic or inorganic anion. Unlike molecular liquids, ionic liquids have a number of advantages determined by the unique combination of their properties such as negligible vapor pressure at room temperature, a stable liquid range of over 300 K, and density being greater than that of water. Therefore, these fluids have been proposed as an attractive alternative to volatile organic compounds (VOCs) for green processes.[1,2]

Ionic liquids have recently gained great attention in a variety of chemical processes. A potential application of ionic liquids is for gas separation processes. The nonvolatility of ionic liquids would not cause any contamination to a gas stream, and thus this feature gives ionic liquids a big advantage over conventional solvents used for absorbing gases. To select an efficient ionic liquid for use as a gas separation medium, it is necessary to know the solubility of the gas in the ionic liquid phase. Brennecke and co-workers[3] proposed a green processing using ionic liquids and a supercritical fluid. They reported that it was possible to extract a desired solute from an ionic liquid using a supercritical fluid without any contamination of the extracted solute with the ionic liquid solvent. They also investigated the use of supercritical carbon dioxide for separating ionic liquids from their organic solvents.[4,5] Such investigations are composed of a complete understanding and designing of processes involving both ionic liquids and supercritical fluids. The most important one for this purpose is to know the phase behavior of ionic liquids + supercritical fluids. Peters and co-workers[6−9] studied the high-pressure phase behavior of binary mixtures consisting of CO_2 and imidazolium-based ionic liquids ([$C_n$mim][PF_6] and [$C_n$mim][BF_4]) in a wide range of solute concentration and at pressures up to about 100 MPa. Blanchard et al.[10] and Aki et al.[11] presented the high-pressure phase behavior of CO_2 with different imidazolium-based ionic liquids and showed the effect of systematically changing the anionic and cationic components of the ionic liquid on the CO_2 + ionic liquid phase behavior. It was reported that large quantities of CO_2 dissolved into the ionic liquid phase, but no appreciable amount of ionic liquid solubilized into the CO_2 phase.[10,11] Even though there are many data available for the ionic liquids with the [PF_6] and [BF_4] anions from the literature, the high-pressure data for the imidazolium-based ionic liquids with the trifluoromethanesulfonate ([TfO]) anion are still rare. In addition to experimental studies, some research groups reported the modeling results for the phase behavior of gas + ionic liquid systems using equations of state.[12−14]

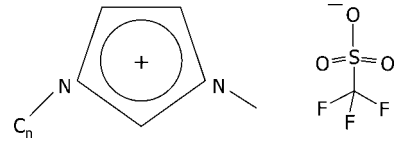

Figure 1. Chemical structure of [$C_n$mim][TfO].

In this work, the solubilities of CO_2 in several imidazolium-based ionic liquids with the [TfO] anion were measured using a high-pressure equilibrium apparatus equipped with a variable-volume view cell. The solubility determination was based on the measurement of bubble pressure for a mixture of CO_2 and ionic liquid with a known composition at a fixed temperature. The CO_2 solubilities in the ionic liquid were measured as a function of temperature and pressure. The experimental data for the binary systems of CO_2 + ionic liquids were correlated using the Peng−Robinson equation of state with the two adjustable binary interaction parameters in its mixing rules.

Experimental Section

Materials. The ionic liquids [$C_n$mim][TfO] were purchased from C-TRI (Korea). The mass fraction purities of [C_2mim][TfO] (CAS registry number: 145022-44-2), [C_4mim][TfO] (CAS registry number: 174899-66-2), [C_6mim][TfO] (CAS registry number: 460345-16-8), and [C_8mim][TfO] (CAS registry number: 403842-84-2) are 99.3 %, 99.6 %, 99.6 %, and 99.5 %, respectively. The purity data by the HPLC analysis were provided by the supplier. The chemical structure of [$C_n$mim][TfO] is shown in Figure 1. The ionic liquid sample was placed into the equilibrium cell for solubility measurements and evacuated by use of a mechanical pump at room temperature for several days. Coulometric Karl Fischer titration (Metrohm model 684) was performed on a sample

* Corresponding author. E-mail: bclee@hannam.ac.kr.

10.1021/je8000443 CCC: $40.75 © 2008 American Chemical Society
Published on Web 11/07/2008

Table 1. Critical Properties and Acentric Factor of Ionic Liquids Estimated from the Method of Joback[18]

ionic liquids	T_c/K	P_c/MPa	ω
[C_2mim][TfO]	756.89	3.48	0.783
[C_4mim][TfO]	796.73	2.81	0.879
[C_6mim][TfO]	837.50	2.31	0.963
[C_8mim][TfO]	879.60	1.94	1.031

of the evacuated ionic liquid. The water mass fraction was about $54 \cdot 10^{-6}$ for [C_2mim][TfO], $58 \cdot 10^{-6}$ for [C_4mim][TfO], $56 \cdot 10^{-6}$ for [C_6mim][TfO], and $59 \cdot 10^{-6}$ for [C_8mim][TfO]. Carbon dioxide (CO_2) used for the measurements was purchased from Myung Sin General Gas Co. (Korea) and had a high purity of 99.99 %. The ionic liquids and CO_2 gas were used without further purification.

Apparatus and Procedure. A detailed description of the experimental apparatus and procedure is given in our previous publications.[15−18] A main feature of using the variable-volume cell apparatus is that the concentration of the system is kept constant during the experiment. The apparatus consists of a view cell equipped with a sapphire window and a movable piston, a pressure generator (High Pressure Equipment Co. model 50-6-15), a borescope (Olympus model R080-044-000-50), a magnetic stirring system, and an air bath. The cylindrical view cell has dimensions of 16 mm i.d. by 70 mm o.d. and an internal working volume of about 31 cm^3. The system pressure is measured with a high-precision pressure gauge (Dresser Heise model CC-12-G-A-02B, ± 0.05 MPa accuracy, ± 0.01 MPa resolution). The system temperature is measured to within ± 0.1 K by an RTD probe inserted into the cell.

The solubilities of CO_2 in the ionic liquid phase were determined by measuring bubble pressures of the CO_2 + ionic liquid mixtures of different compositions at known temperatures using the variable-volume view cell apparatus. The experiment was performed by the following procedure. A known mass (about 8 g) of ionic liquid sample was loaded into the cell. The transfer of the ionic liquid into the view cell was conducted in the following way. The ionic liquid sample was dried by evacuation at room temperature and kept in a vial with a silicon septum cap. The dried ionic liquid sample was taken using a gastight syringe and then injected into the cell. After assembling a piston, o-rings, and a sapphire window in the view cell, the cell was then placed inside the air bath. The amount of the ionic liquid loaded was determined by using a sensitive balance (AND model HM-30) measurable to ± 0.1 mg. To remove any entrapped air present in the cell and any dissolved gas and water in the ionic liquid, the cell was evacuated overnight at room temperature using a mechanical pump; the ultimate pressure during evacuation was about 0.5 Pa. Therefore, the ionic liquid sample was always kept dried in the cell.

Once the vapor space of the system was fully evacuated, a known mass of CO_2 was charged into the cell through a feed line. The exact amount of CO_2 gas introduced into the cell was determined by weighing the CO_2 sample cylinder before and after loading using a balance (Precisa model 1212 M) with an accuracy of ± 1 mg. To prevent any loss of CO_2 gas in the feed line during loading, the CO_2 gas in the feed line was recovered back into the CO_2 sample cylinder by dipping the cylinder into a Dewar flask filled with liquid nitrogen. The uncertainties in measuring ionic liquid and CO_2 are 0.2 mg and 2 mg, respectively. The uncertainty analysis for the composition measurement for each component was performed in accordance with the ISO guideline.[19]

The pressure was varied until a phase change was visually observed for a mixture with a constant overall composition. To dissolve the CO_2 gas into the ionic liquid, the fluid in the cell was compressed by moving the piston located within the cell using the pressure generator. The liquid was well agitated by a magnetic stirrer. At the same time, the system was heated to a desired temperature. The temperature was controlled with an uncertainty of ± 0.1 K. As the pressure increased, the CO_2 gas dissolved into the ionic liquid phase, and finally the fluid became a single homogeneous phase. Once the system reached thermal equilibrium and the fluid was maintained at a homogeneous single phase, the pressure was then slowly reduced at about 0.5 MPa/min until tiny CO_2 bubbles started to form from the single-phase solution. The initial pressure at which the first bubbles are observed is the bubble pressure of the solution at a given composition and temperature. Every measurement was repeated at least twice at each temperature. The uncertainty in the bubble point pressure was 0.02 MPa. The cloud point behavior was observed rather than the bubble point behavior for a solution of very high CO_2 mole fractions. At the cloud point, the solution becomes cloudy due to the phase transition from a single to a liquid + liquid phase. In our experiments, the cloud pressure was defined as the pressure at which it was no longer possible to visually observe the stirring bar in the cell.[16] The bubble or point pressures at different temperatures and compositions were measured in the same way, thus creating pressure−temperature (P, T) isopleths.

Modeling. For a gas (1) + ionic liquid (2) system, the ionic liquid is taken to be nonvolatile, and only pure gas exists in the gas phase. The condition for the phase equilibrium is satisfied when the fugacities of the gas component have equal values in both phases at a constant temperature and pressure

$$f_1^{\text{gas}} = \hat{f}_1^{\text{IL}} \tag{1}$$

where f_1^{gas} is the fugacity of gas in the pure gas phase and $\hat{f}_1^{\text{IL}}$ is the fugacity of gas in the ionic liquid phase. The relationship of fugacity with temperature and pressure can be expressed by an equation of state. Among the numerous equations of state, the Peng−Robinson equation of state (PR-EoS) is one of the most popular for practical applications.

The original PR-EoS[20] is expressed as

$$P = \frac{RT}{V-b} - \frac{a(T)}{V(V+b)+b(V-b)} \tag{2}$$

The mixture parameters in the ionic liquid phase are calculated from the following quadratic mixing rules

$$a = \sum_i \sum_j x_i x_j a_{ij} \tag{3}$$

$$a_{ij} = (a_{ii}a_{jj})^{1/2}(1-k_{ij}) \tag{4}$$

$$b = \sum_i \sum_j x_i x_j b_{ij} \tag{5}$$

$$b_{ij} = \left(\frac{b_i + b_j}{2}\right)(1-l_{ij}) \tag{6}$$

In eq 5, $b_{ii} = b_i$ and $b_{jj} = b_j$. k_{ij} and l_{ij} in eq 4 and eq 6 are the binary interaction parameters. The EoS parameters for pure component i are the same as found in all the textbooks of classical thermodynamics. The expressions for the fugacities of the gas component in gas and ionic liquid phases are also available from the literature.[20]

Information on the critical properties and acentric factor is needed to utilize the PR-EoS. Those properties are readily available for CO_2, but they are not available for the ionic liquids. Therefore, those properties for the ionic liquids were estimated using Joback's group contribution method.[21] The group identities

Table 2. Experimental Bubble Point or Cloud Point Data for Various CO_2 Mole Fractions (x_1) in the CO_2 (1) + [C_2mim][TfO] (2) System

		T = 303.85 K		T = 314.05 K		T = 324.15 K	
x_1	δx_1[a]	P/MPa	P^{calc}/MPa[b]	P/MPa	P^{calc}/MPa	P/MPa	P^{calc}/MPa
0.1794	0.0017	0.80 (b[c])	0.75	1.00 (b)	0.91	1.15 (b)	1.07
0.2613	0.0032	1.50 (b)	1.37	1.80 (b)	1.68	2.20 (b)	1.98
0.3546	0.0043	2.35 (b)	2.38	2.80 (b)	2.94	3.25 (b)	3.52
0.4141	0.0053	3.10 (b)	3.22	3.90 (b)	4.02	4.80 (b)	4.88
0.4670	0.0061	3.78 (b)	4.13	4.80 (b)	5.22	6.00 (b)	6.45
0.5078	0.0069	4.60 (b)	4.96	5.80 (b)	6.38	7.50 (b)	8.06
0.5435	0.0076	5.35 (b)	5.80	7.20 (b)	7.69	9.60 (b)	10.18
0.5681	0.0083	5.90 (b)	6.49	8.60 (b)	9.12	12.30 (c)	12.93
0.5975	0.0088	7.60 (c[d])	8.16	13.80 (c)	13.32	19.60 (c)	18.31
0.6151	0.0094	12.00 (c)	11.18	17.50 (c)	17.04	23.10 (c)	22.55
0.6268	0.0101	14.90 (c)	13.67	21.00 (c)	19.93	27.00 (c)	25.78

		T = 334.35 K		T = 344.55 K	
x_1	δx_1	P/MPa	P^{calc}/MPa	P/MPa	P^{calc}/MPa
0.1794	0.0017	1.30(b)	1.25	1.55(b)	1.52
0.2613	0.0032	2.50(b)	2.34	3.05(b)	2.83
0.3546	0.0043	4.10(b)	4.20	5.00(b)	5.08
0.4141	0.0053	5.85(b)	5.88	7.10(b)	7.14
0.4670	0.0061	7.50(b)	7.90	9.20(b)	9.71
0.5078	0.0069	9.50(b)	10.11	11.90(b)	12.68
0.5435	0.0076	12.70(b)	13.32	16.50(b)	16.90
0.5681	0.0083	16.30(c)	16.97	20.80(c)	21.16
0.5975	0.0088	24.50(c)	23.15	29.00(c)	27.88
0.6151	0.0094	28.50(c)	27.80	33.30(c)	32.80
0.6268	0.0101	32.60(c)	31.30	37.80(c)	36.45

[a] Uncertainty in x_1. [b] Pressure calculated by the Peng−Robinson EoS. [c] Bubble pressure behavior observed. [d] Cloud pressure behavior observed.

Table 3. Experimental Bubble Point or Cloud Point Data for Various CO_2 Mole Fractions (x_1) in the CO_2 (1) + [C_4mim][TfO] (2) system

		T = 303.85 K		T = 314.05 K		T = 324.15 K	
x_1	δx_1[a]	P/MPa	P^{calc}/MPa[b]	P/MPa	P^{calc}/MPa	P/MPa	P^{calc}/MPa
0.2182	0.0037	0.85 (b[c])	0.83	1.02 (b)	0.95	1.15 (b)	1.16
0.2734	0.0052	1.15 (b)	1.23	1.30 (b)	1.41	1.75 (b)	1.73
0.3344	0.0064	1.70 (b)	1.78	2.05 (b)	2.07	2.65 (b)	2.53
0.3786	0.0076	2.30 (b)	2.26	2.65 (b)	2.66	3.20 (b)	3.26
0.4140	0.0087	2.95 (b)	2.72	3.30 (b)	3.23	3.90 (b)	3.95
0.4574	0.0014	3.40 (b)	3.35	4.30 (b)	4.03	5.30 (b)	4.96
0.4929	0.0026	3.90 (b)	3.95	4.90 (b)	4.81	6.10 (b)	5.96
0.5367	0.0036	4.90 (b)	4.81	5.90 (b)	5.97	7.30 (b)	7.50
0.5761	0.0045	6.00 (b)	5.72	7.20 (b)	7.31	8.70 (b)	9.48
0.6134	0.0052	6.80 (b)	6.81	8.60 (b)	9.58	12.30 (b)	13.38
0.6325	0.0057	8.50 (c[d])	8.15	13.50 (c)	12.46	18.20 (c)	16.84
0.6537	0.0010	12.00 (c)	12.08	17.50 (c)	17.07	22.70 (c)	21.85
0.6720	0.0018	16.00 (c)	16.63	22.00 (c)	22.15	27.40 (c)	27.17

		T = 334.35 K		T = 344.55 K	
x_1	δx_1	P/MPa	P^{calc}/MPa	P/MPa	P^{calc}/MPa
0.2182	0.0037	1.35(b)	1.43	1.90(b)	1.78
0.2734	0.0052	2.30(b)	2.11	2.80(b)	2.62
0.3344	0.0064	3.20(b)	3.09	3.70(b)	3.80
0.3786	0.0076	3.90(b)	3.98	4.75(b)	4.89
0.4140	0.0087	4.75(b)	4.83	5.50(b)	5.93
0.4574	0.0014	6.40(b)	6.09	7.80(b)	7.48
0.4929	0.0026	7.60(b)	7.36	9.00(b)	9.09
0.5367	0.0036	9.20(b)	9.42	11.20(b)	11.80
0.5761	0.0045	11.40(b)	12.37	14.70(b)	15.75
0.6134	0.0052	16.60(b)	17.61	21.50(c)	21.87
0.6325	0.0057	23.40(c)	21.55	28.00(c)	26.11
0.6537	0.0010	28.00(c)	26.97	33.30(c)	31.77
0.6720	0.0018	32.40(c)	32.61	37.50(c)	37.55

[a] Uncertainty in x_1. [b] Pressure calculated by the Peng−Robinson EoS. [c] Bubble pressure behavior observed. [d] Cloud pressure behavior observed.

and their Joback's values for contributions to the critical properties are available from the literature.[21] The normal boiling temperature required to estimate the critical temperature was also estimated from Joback's method. The acentric factors of the ionic liquids were estimated by the Ambrose−Walton corresponding-states method.[21] The critical properties and acentric factors of the ionic liquids [$C_n$mim][TfO] are listed in Table 1.

For a CO_2 + ionic liquid system, at a given temperature and CO_2 mole fraction (x_1), the equilibrium pressures (P) were calculated, which satisfied the equilibrium relation (eq 1). The volumetric properties of gas and ionic liquid phases, which were necessary to calculate the fugacities of gas in gas and ionic liquid phases, were obtained by solving the PR-EoS (eq 2). A nonlinear least-squares method was used to solve this problem. The same calculations were repeated at different CO_2 mole fractions, and finally a P, x_1 diagram was completed.

Before performing the equilibrium calculations described above using the PR-EoS, the adjustable binary interaction parameters (k_{12} and l_{12}) were determined first for each system.

Table 4. Experimental Bubble Point or Cloud Point Data for Various CO_2 Mole Fractions (x_1) in the CO_2 (1) + [C_6mim][TfO] (2) System

		T = 303.85 K		T = 314.05 K		T = 324.15 K	
x_1	δx_1[a]	P/MPa	P^{calc}/MPa[b]	P/MPa	P^{calc}/MPa	P/MPa	P^{calc}/MPa
0.2885	0.0019	1.25 (b[c])	1.02	1.65 (b)	1.28	2.00 (b)	1.62
0.3566	0.0035	1.70 (b)	1.55	2.10 (b)	1.94	2.70 (b)	2.44
0.4162	0.0048	2.15 (b)	2.15	2.65 (b)	2.69	3.40 (b)	3.37
0.4632	0.0060	2.70 (b)	2.73	3.20 (b)	3.42	4.00 (b)	4.27
0.5329	0.0067	3.20 (b)	3.80	4.20 (b)	4.80	5.20 (b)	6.00
0.5626	0.0076	4.00 (b)	4.35	5.00 (b)	5.52	6.50 (b)	6.94
0.5898	0.0085	4.50 (b)	4.90	5.50 (b)	6.28	7.00 (b)	7.97
0.6110	0.0093	4.90 (b)	5.38	6.20 (b)	6.97	8.00 (b)	8.96
0.6236	0.0011	5.50 (b)	5.69	7.40 (b)	7.44	9.40 (b)	9.71
0.6487	0.0021	6.00 (b)	6.38	9.20 (b)	8.68	12.50 (b)	11.94
0.6668	0.0031	6.70 (b)	6.98	10.50 (b)	10.53	14.30 (b)	14.52
0.6887	0.0039	8.50 (c[d])	9.37	14.00 (c)	14.39	19.00 (c)	18.77
0.7059	0.0046	14.60 (c)	12.99	19.60 (c)	18.48	24.50 (c)	23.01
0.7171	0.0053	18.00 (c)	15.90	23.30 (c)	21.65	28.20 (c)	26.20

		T = 334.35 K		T = 344.55 K	
x_1	δx_1	P/MPa	P^{calc}/MPa	P/MPa	P^{calc}/MPa
0.2885	0.0019	2.30(b)	1.94	2.80(b)	2.33
0.3566	0.0035	3.30(b)	2.91	3.90(b)	3.48
0.4162	0.0048	4.10(b)	4.02	4.80(b)	4.80
0.4632	0.0060	4.85(b)	5.11	5.80(b)	6.10
0.5329	0.0067	6.50(b)	7.24	8.00(b)	8.70
0.5626	0.0076	7.80(b)	8.44	9.50(b)	10.21
0.5898	0.0085	8.50(b)	9.81	10.50(b)	11.97
0.6110	0.0093	9.80(b)	11.21	11.90(b)	13.77
0.6236	0.0011	12.00(b)	12.27	15.10(b)	15.09
0.6487	0.0021	15.80(b)	15.18	18.90(b)	18.46
0.6668	0.0031	18.20(b)	18.08	21.90(c)	21.59
0.6887	0.0039	23.50(c)	22.58	28.00(c)	26.24
0.7059	0.0046	28.85(c)	26.91	32.90(c)	30.62
0.7171	0.0053	32.40(c)	30.14	36.30(c)	33.84

[a] Uncertainty in x_1. [b] Pressure calculated by the Peng−Robinson EoS. [c] Bubble pressure behavior observed. [d] Cloud pressure behavior observed.

The experimentally obtained P, x_1 data at a given temperature for a CO_2 + ionic liquid system were correlated with the PR-EoS, and then a set of optimum values of the k_{12} and l_{12} parameters were found by minimizing the following objective function

$$F = \sum_{i=1}^{N} \frac{|P_i^{calc} - P_i|}{P_i} \quad (7)$$

where P_i is the experimental value of pressure; P_i^{calc} is the pressure calculated by the PR-EoS at the experimental value of CO_2 mole fraction; and N is the number of data points. An optimization routine, which solved a nonlinear least-squares problem, was used.

Results and Discussion

The bubble or cloud pressures for the CO_2 + [$C_n$mim][TfO] mixtures of different compositions were measured at five different temperatures: 303.85 K, 314.05 K, 324.15 K, 334.35 K, and 344.55 K. The experimental data are given in Tables 2 to 5. As a graphical representation of the data, the P, T isopleths for the CO_2 + [C_2mim][TfO] system are shown in Figure 2. The solubility results are given in terms of the mole fraction of CO_2 (component 1) in the ionic liquid (component 2) phase, x_1. The uncertainty (δx_1) in the CO_2 mole fraction for each point is also shown in Tables 2 to 5. The average uncertainty values in the CO_2 mole fraction were estimated to be 0.0065 for the CO_2 + [C_2mim][TfO] system, 0.0052 for the CO_2 + [C_4mim][TfO] system, 0.0049 for the CO_2 + [C_6mim][TfO] system, and 0.0081 for the CO_2 + [C_8mim][TfO] system. Overall, the average uncertainty in the CO_2 mole fraction for all the systems was about 0.0061. The equilibrium pressure increased with an increase in the system temperature at a fixed CO_2 mole fraction. Tables 2 to 5 also show the results of phase change behavior observed during the experiments. As indicated in the tables, for a solution of very high CO_2 mole fraction, the cloud pressure behavior was observed rather than the bubble pressure behavior.

When the CO_2 mole fraction increased isothermally, the bubble or cloud pressure increased significantly. This can be more easily seen from a P, x_1 diagram in which the equilibrium pressure is plotted against the CO_2 mole fraction at various temperatures. As an example, Figure 3 shows the P, x_1 diagram at the five different temperatures described above for the CO_2 + [C_4mim][TfO] systems. The solubilities of CO_2 in ionic liquids are illustrated as a function of pressure at different temperatures. The equilibrium pressures were reasonably low at lower mole fractions of CO_2. However, when the CO_2 mole fraction further increased, the equilibrium pressures increased dramatically. The solubility of CO_2 in the ionic liquid decreased with an isobaric increase in temperature, and the effect of temperature on CO_2 solubility was larger at higher CO_2 mole fractions. When the CO_2 mole fraction in the ionic liquid phase is low, CO_2 can dissolve very well into the ionic liquid, and thus a large pressure increase does not occur with increasing CO_2 mole fraction. At higher mole fractions of CO_2, however, the CO_2 solubility does not increase much even for a very large pressure increase since it approaches its maximum value.

The cloud pressure behavior was observed instead of the bubble pressure behavior when the sharp increase of equilibrium pressure with the increase of CO_2 solubility occurred at high CO_2 mole fractions. This phenomenon can be seen by comparing the phase behavior data in Tables 2 to 5 with the corresponding P, x_1 diagrams for each CO_2 + ionic liquid system. When the CO_2 solubility in ionic liquid is measured in our experiments, the pressure is slowly reduced until the phase separation occurs

Table 5. Experimental Bubble Point or Cloud Point Data for Various CO_2 Mole Fractions (x_1) in the CO_2 (1) + [C_8mim][TfO] (2) System

		T = 303.85 K		T = 314.05 K		T = 324.15 K	
x_1	δx_1[a]	P/MPa	P^{calc}/MPa[b]	P/MPa	P^{calc}/MPa	P/MPa	P^{calc}/MPa
0.2166	0.0022	0.68 (b[c])	0.66	0.80 (b)	0.80	1.08 (b)	1.04
0.3445	0.0039	1.58 (b)	1.49	1.90 (b)	1.80	2.35 (b)	2.27
0.4377	0.0051	2.48 (b)	2.40	3.00 (b)	2.91	3.70 (b)	3.62
0.4896	0.0063	2.98 (b)	3.05	3.80 (b)	3.70	4.70 (b)	4.60
0.5508	0.0071	3.80 (b)	3.97	4.75 (b)	4.86	5.80 (b)	6.04
0.5780	0.0081	4.25 (b)	4.44	5.30 (b)	5.47	6.55 (b)	6.81
0.6105	0.0089	4.75 (b)	5.07	6.00 (b)	6.31	7.50 (b)	7.92
0.6414	0.0095	5.40 (b)	5.75	6.90 (b)	7.27	8.60 (b)	9.27
0.6703	0.0099	6.40 (b)	6.49	7.90 (b)	8.48	10.60 (b)	11.29
0.6918	0.0104	6.90 (b)	7.19	10.00 (c)	10.34	13.60 (c)	13.83
0.7162	0.0107	10.00 (c[d])	10.52	14.00 (c)	14.33	18.00 (c)	18.02
0.7321	0.0111	14.30 (c)	14.02	18.50 (c)	17.90	22.40 (c)	21.52
0.7414	0.0116	18.00 (c)	16.48	22.00 (c)	20.36	25.80 (c)	23.87

		T = 334.35 K		T = 344.55 K	
x_1	δx_1	P/MPa	P^{calc}/MPa	P/MPa	P^{calc}/MPa
0.2166	0.0022	1.35(b)	1.27	1.65(b)	1.51
0.3445	0.0039	2.85(b)	2.75	3.35(b)	3.24
0.4377	0.0051	4.45(b)	4.37	5.20(b)	5.15
0.4896	0.0063	5.50(b)	5.55	6.40(b)	6.55
0.5508	0.0071	6.90(b)	7.32	8.30(b)	8.69
0.5780	0.0081	7.85(b)	8.30	9.20(b)	9.90
0.6105	0.0089	9.40(b)	9.74	11.10(b)	11.73
0.6414	0.0095	10.90(b)	11.62	13.20(b)	14.10
0.6703	0.0099	13.60(c)	14.32	16.40(c)	17.26
0.6918	0.0104	17.00(c)	17.21	20.20(c)	20.40
0.7162	0.0107	21.70(c)	21.57	25.30(c)	24.90
0.7321	0.0111	26.10(c)	25.08	29.90(c)	28.44
0.7414	0.0116	29.80(c)	27.40	34.00(c)	30.74

[a] Uncertainty in x_1. [b] Pressure calculated by the Peng−Robinson EoS. [c] Bubble pressure behavior observed. [d] Cloud pressure behavior observed.

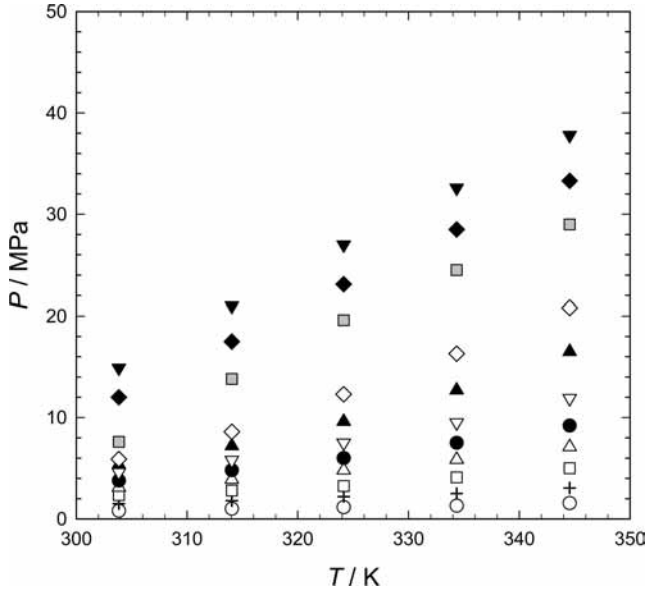

Figure 2. P, T isopleths of the C_2 (1) + [C_2mim][TfO] (2) mixtures at different CO_2 mole fractions (x_1): ○, 0.1794; +, 0.2613; □, 0.3546; Δ, 0.4141; ●, 0.4670; ▽, 0.5078; ▲, 0.5435; ◇, 0.5681; ■, 0.5975; ♦, 0.6151; ▼, 0.6268.

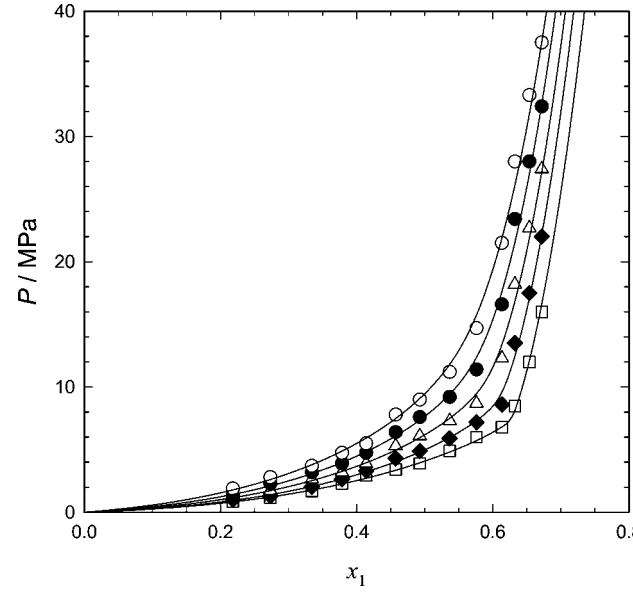

Figure 3. P, x_1 diagram of the CO_2 (1) + [C_4mim][TfO] (2) mixtures at different temperatures: □, 303.85 K; ♦, 314.05 K; Δ, 324.15 K; ●, 334.35 K; ○, 344.55 K. The lines are the calculations by the PR-EoS model. The binary interaction parameters for each temperature are listed in Table 6.

from the single-phase solution where CO_2 is dissolved in the ionic liquid phase. When the CO_2 mole fraction in the solution is small and the equilibrium pressure is low, CO_2 behaves as gas, and thus the tiny bubbles come out of the solution with the pressure decrease even at temperatures above the critical point of CO_2. However, at higher CO_2 mole fractions and higher pressure, CO_2 behaves like a liquid, and the cloud pressure behavior is observed with a decrease of the equilibrium pressure. It is acknowledged that the high density of the CO_2 phase makes the demixing appear closer to liquid−liquid equilibrium behavior than to vapor−liquid equilibrium behavior. At 303.85 K, which is lower than the critical temperature of CO_2, it is shown in Tables 2 to 5 that the cloud pressure behavior was observed instead of the bubble pressure behavior as the system pressure was higher than about 7.38 MPa, which is the critical pressure of CO_2. At those conditions, CO_2 behaves as a liquid in the ionic liquid phase, and thus liquid−liquid equilibrium is formed instead of vapor−liquid equilibrium with a decrease of the equilibrium pressure.

In general, a system in which a large amount of CO_2 dissolves in the liquid phase at low pressures tends to give a simple two-phase envelope with a mixture critical temperature at moderate

Table 6. Binary Interaction Parameters of the PR-EoS Optimized for the CO_2 + [$C_n$mim][TfO] Systems

ionic liquids	binary interaction parameters	T/K 303.85	314.05	324.15	334.35	344.55
[C_2mim][TfO]	k_{12}	0.0914	0.1003	0.1101	0.1194	0.1262
	l_{12}	0.0757	0.0807	0.0876	0.0933	0.0942
[C_4mim][TfO]	k_{12}	0.0901	0.0989	0.1039	0.1097	0.1136
	l_{12}	0.0713	0.0804	0.0819	0.0828	0.0804
[C_6mim][TfO]	k_{12}	0.0828	0.0873	0.0893	0.0924	0.0948
	l_{12}	0.0727	0.0736	0.0713	0.0727	0.0722
[C_8mim][TfO]	k_{12}	0.0762	0.0784	0.0779	0.0789	0.0806
	l_{12}	0.0553	0.0573	0.0535	0.0524	0.0523

Table 7. Deviations between Experimental and Calculated Values in Equilibrium Pressures for the CO_2 + [$C_n$mim][TfO] Systems

ionic liquids	T/K 303.85	314.05	324.15	334.35	344.55	average
			100 AAD[a]			
[C_2mim][TfO]	7.1	6.0	6.0	4.1	3.3	5.3
[C_4mim][TfO]	3.1	4.0	4.0	4.5	4.4	4.0
[C_6mim][TfO]	8.7	8.0	7.7	7.8	7.3	7.9
[C_8mim][TfO]	4.4	4.0	4.1	4.1	4.8	4.3

[a] Average absolute deviation, which is defined as: AAD = $(1/N)\sum_{i=1}^{N}(|P_i^{calc} - P_i|/P_i)$ (N: number of data).

pressures.[4,7] However, the CO_2 + [$C_n$mim][TfO] systems studied in this work illustrate an almost vertical extension to a very high pressure of the two-phase boundary, instead of having a closed phase envelope. Thus, the phase behavior of the CO_2 + [$C_n$mim][TfO] systems is not common. This kind of phase behavior has already been noticed for other CO_2 + ionic liquid systems such as CO_2 + [$C_n$mim][PF_6],[6,7] CO_2 + [$C_n$mim][BF_4],[8,9] and CO_2 + [$C_n$mim][Tf_2N].[17,18]

The PR-EoS with the quadratic mixing rules was used to describe the experimental data of the solubility of CO_2 in [$C_n$mim][TfO]. The two binary interaction parameters in the mixing rules were optimized using the P, x_1 data for each system. Table 6 summarizes the binary interaction parameters at four different temperatures for each system. The calculated results are given in Tables 2 to 5. Figure 3 shows the graphical representation of the modeling results along with the experimental data for the CO_2 + [C_4mim][TfO] system. Other systems show similar results as well. The modeling results using the PR-EoS are summarized in Table 7. The average absolute deviations (AAD) between the calculated and experimental equilibrium pressures were calculated for each system and temperature. The AAD values were all less than 10 %, as shown in Table 7. It can be concluded that the PR-EoS can satisfactorily model the high-pressure solubility of CO_2 in [$C_n$mim][TfO] over a wide range of pressure up to the supercritical region of CO_2.

Figure 4 compares the solubility data for the CO_2 + [$C_n$mim][TfO] systems at 324.15 K and shows the influence of structural variations in the imidazolium cation on the CO_2 solubility for the [TfO] anion-based ionic liquids. The solubilities of CO_2 in [$C_n$mim][TfO] were nearly the same at lower pressures, while they differed greatly at elevated pressures. In the high-pressure range, the CO_2 solubility increased as the length of the 1-alkyl chain in the cation of [$C_n$mim][TfO] increased.

A quantitative comparison of our data with those by other research groups was given. Aki et al.[11] reported the high-pressure phase behavior of CO_2 with various imidazolium-based ionic liquids. CO_2 solubilities were measured in a stoichiometric phase equilibrium apparatus with a cathetometer to determine the liquid volume in a view cell. Figure 5 shows the comparison of the CO_2 solubilities in [C_4mim][TfO]. The CO_2 solubilties

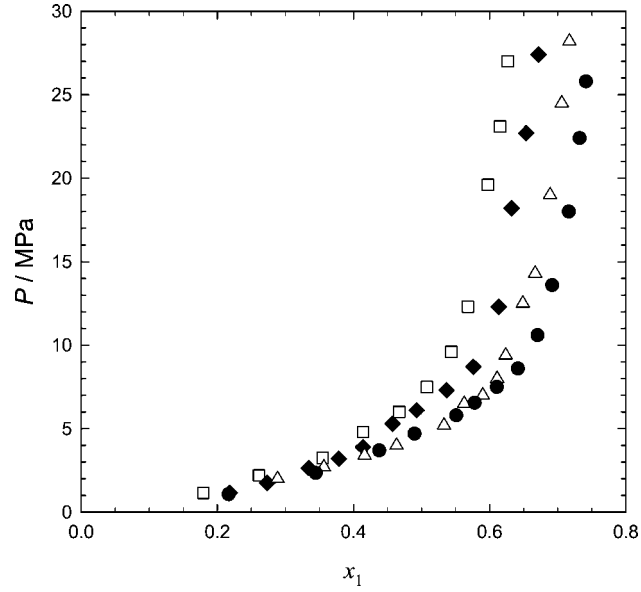

Figure 4. Comparison of solubilities of CO_2 in ionic liquids [$C_n$mim][TfO] at 324.15 K: □, [C_2mim][TfO]; ♦, [C_4mim][TfO]; Δ, [C_6mim][TfO]; ●, [C_8mim][TfO].

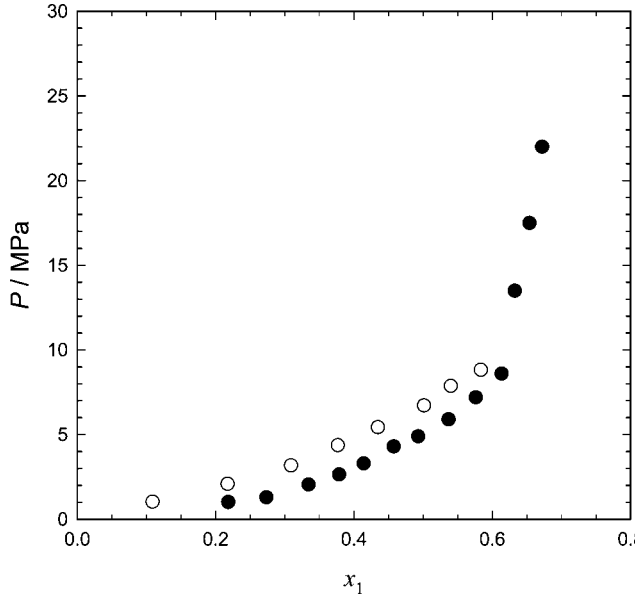

Figure 5. Comparison of solubilities of CO_2 in [C_4mim][TfO]: ●, our data at 314.05 K; ○, data from Aki et al.[11] at 313.2 K.

from our work were about 20 % higher than those from Aki et al.,[11] when compared at the same equilibrium pressures.

Figure 6 compares the CO_2 solubilities in the [C_6mim]-based ionic liquids with four different anions at 324.15 K, showing the effect of anion on the CO_2 solubility. The data show the similarities in phase behavior; in all those binary systems, the equilibrium pressure increased very sharply at high CO_2 mole fractions. [C_6mim][Tf_2N] gave the highest CO_2 solubilities, when compared at the same pressure. The solubilities of CO_2 in the ionic liquids with the [PF_6] and [BF_4] anions were almost the same. The anion appears to play a significant role in determining the CO_2 solubility. Cadena et al.[22] showed in their molecular simulations for CO_2 + ionic liquid mixtures that CO_2 associated with the anion, positioning itself to maximize favorable interactions. The strength of these interactions of CO_2 with [TfO] and [Tf_2N] may simply be stronger than those with [PF_6] and [BF_4]. As shown in Figure 6, CO_2 had higher

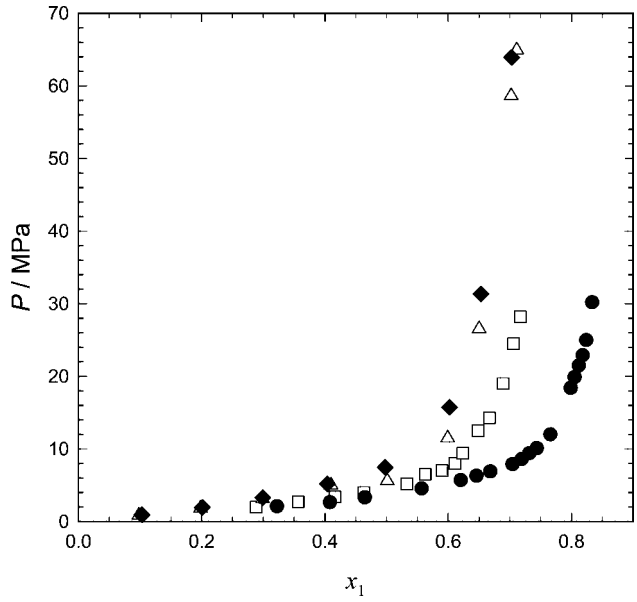

Figure 6. Comparison of solubilities of CO_2 in the [C_6mim]-based ionic liquids with different anions at 324.15 K: □, [C_6mim][TfO]; ●, [C_6mim][Tf_2N] (data from Shin et al.[15]); Δ, [C_6mim][PF_6] (data estimated from Shariati and Peters[6]); ♦, [C_6mim][BF_4] (data estimated from Costantini et al.[8]).

solubilities in ionic liquids with the [TfO] and [Tf_2N] anions containing a fluoroalkyl group (CF_3) than in the two ionic liquids with inorganic fluorinated anions, [PF_6] and [BF_4]. Therefore, the higher solubility of CO_2 in the [C_6mim][TfO] and [C_6mim][Tf_2N] ionic liquids can be attributed to the fluoroalkyl group present in the [TfO] and [Tf_2N] anions. It is well-known that fluoroalkyl groups are CO_2-philic, although the exact mechanism of this phenomenon is poorly understood. [C_6mim]-[Tf_2N] gave a higher CO_2 solubility than [C_6mim][TfO], as shown in Figure 6. That is probably because the [Tf_2N] anion has more fluoroalkyl groups than the [TfO] anion.

Conclusions

The solubilities of CO_2 in the ionic liquids [$C_n$mim][TfO] (n = 2, 4, 6, 8) were determined by measuring the bubble point or cloud point pressures of the binary mixtures using a high-pressure equilibrium apparatus equipped with a variable-volume view cell. The experimental results showed that CO_2 gave very high solubilities in the ionic liquids at lower pressures, while the equilibrium pressure increased very steeply at higher concentrations of CO_2. The solubility of CO_2 in the ionic liquids decreased with an increase in temperature. The Peng−Robinson equation of state with two binary interaction parameters in its quadratic mixing rules was capable of satisfactorily modeling the high-pressure solubility of CO_2 in [$C_n$mim][TfO] over a wide range of pressures up to the supercritical region of CO_2. Variation of the length of the 1-alkyl chain in the cation of [$C_n$mim][TfO] was found to have a large effect on the CO_2 solubility. The solubilities of CO_2 in [$C_n$mim][TfO] were nearly the same at lower pressures, but in the high-pressure range the CO_2 solubility increased with the increase of the length of 1-alkyl chain in the cation of [$C_n$mim][TfO].

Literature Cited

(1) Brennecke, J. F.; Maginn, E. J. Ionic Liquids: Innovative Fluids for Chemical Processing. *AIChE J.* **2001**, *47*, 2384–2389.
(2) DeSimone, J. M. Practical Approaches to Green Solvents. *Science* **2002**, *297*, 799–803.
(3) Blanchard, L. A.; Hancu, D.; Beckman, E. J.; Brennecke, J. F. Green Processing Using Ionic Liquids and CO_2. *Nature* **1999**, *399*, 28–29.
(4) Blanchard, L. A.; Brennecke, J. F. Recovery of Organic Products from Ionic Liquids Using Supercritical Carbon Dioxide. *Ind. Eng. Chem. Res.* **2001**, *40*, 287–292.
(5) Scurto, A. M.; Aki, S. N. V. K.; Brennecke, J. F. CO_2 as a Separation Switch for Ionic Liquid/Organic Mixtures. *J. Am. Chem. Soc.* **2002**, *124*, 10276–10277.
(6) Shariati, A.; Peters, C. J. High-Pressure Phase Equilibria of Systems with Ionic Liquids. Part III. The Binary System Carbon Dioxide + 1-Hexyl-3-methylimidazolium Hexafluorophosphate. *J. Supercrit. Fluids* **2004**, *30*, 139–144.
(7) Shariati, A.; Gutkowski, K.; Peters, C. J. Comparison of the Phase Behavior of Some Selected Binary Systems with Ionic Liquids. *AIChE J.* **2005**, *51*, 1532–1540.
(8) Costantini, M.; Toussaint, V. A.; Shariati, A.; Peters, C. J.; Kikic, I. High-Pressure Phase Behavior of Systems with Ionic Liquids: Part IV. Binary System Carbon Dioxide + 1-Hexyl-3-methylimidazolium Tetrafluoroborate. *J. Chem. Eng. Data* **2005**, *50*, 52–55.
(9) Kroon, M.; Shariati, A.; Costantini, M.; van Spronsen, J.; Witkamp, G.-J.; Sheldon, R. A.; Peters, C. J. High-Pressure Phase Behavior of Systems with Ionic Liquids: Part V. The Binary System Carbon Dioxide + 1-Butyl-3-methylimidazolium Tetrafluoroborate. *J. Chem. Eng. Data* **2005**, *50*, 173–176.
(10) Blanchard, L. A.; Gu, Z.; Brennecke, J. F. High-Pressure Phase Behavior of Ionic Liquid/CO_2 Systems. *J. Phys. Chem. B* **2001**, *105*, 2437–2444.
(11) Aki, S. N. V. K.; Mellein, B. R.; Saurer, E. M.; Brennecke, J. F. High-Pressure Phase Behavior of Carbon Dioxide with Imidazolium-Based Ionic Liquids. *J. Phys. Chem. B* **2004**, *108*, 20355–20365.
(12) Shariati, A.; Peters, C. J. High-Pressure Phase Behavior of Systems with Ionic Liquids: Measurements and Modeling of the Binary System Fluoroform + 1-Ethyl-3-methylimidazolium Hexafluorophosphate. *J. Supercrit. Fluids* **2003**, *25*, 109–117.
(13) Shiflett, M. B.; Yokozeki, A. Solubilities and Diffusivities of Carbon Dioxide in Ionic Liquids: [bmim][PF_6] and [bmim][BF_4]. *Ind. Eng. Chem. Res.* **2005**, *44*, 4453–4464.
(14) Liu, Z.; Wu, W.; Han, B.; Dong, Z.; Zhao, G.; Wang, J.; Jiang, T.; Yang, G. Study on the Phase Behaviors, Viscosities, and Thermodynamic Properties of CO_2/[C_4mim][PF_6]/ Methanol System at Elevated Pressures. *Chem.−Eur. J.* **2003**, *9*, 3897–3903.
(15) Lee, J. M.; Lee, B.-C.; Cho, C.-H. Measurement of Bubble Point Pressures and Critical Points of Carbon Dioxide and Chlorodifluoromethane Mixtures Using the Variable-Volume View Cell Apparatus. *Korean J. Chem. Eng.* **2000**, *17*, 510–515.
(16) Lee, J. M.; Lee, B.-C.; Lee, S.-H. Cloud Points of Biodegradable Polymers in Compressed and Supercritical Chlorodifluoromethane. *J. Chem. Eng. Data* **2000**, *45*, 851–856.
(17) Oh, D.-J.; Lee, B.-C. High-Pressure Phase Behavior of Carbon Dioxide in Ionic Liquid 1-Butyl-3-methylimidazolium Bis(trifluoromethylsulfonyl)imide. *Korean J. Chem. Eng.* **2006**, *23*, 800–805.
(18) Shin, E.-K.; Lee, B.-C.; Lim, J. S. High-Pressure Solubilities of Carbon Dioxide in Ionic Liquids: 1-Alkyl-3-methylimidazolium Bis(trifluoromethylsulfonyl)imide. *J. Supercrit. Fluids* **2008**, *45*, 282–292.
(19) International Organization of Standardization (ISO) . *Guide to the Expression of Uncertainty in Measurement*; ISO: Geneva, Switzerland, 1995.
(20) Prausnitz, J. M.; Lichtenthaler, R. N.; de Azevedo, E. G. *Molecular Thermodynamics of Fluid-Phase Equilibria*, 3rd ed.; Prentice-Hall: NJ, 1999.
(21) Poling, B. E.; Prausnitz, J. M.; O'Connell, J. P. *The Properties of Gases and Liquids*, 5th ed.; McGraw-Hill: NY, 2001.
(22) Cadena, C.; Anthony, J. L.; Shah, J. K.; Morrow, T. I.; Brennecke, J. F. Why is CO_2 So Soluble in Imidazolium-Based Ionic Liquid. *J. Am. Chem. Soc.* **2004**, *126*, 5300–5308.

Received for review January 16, 2008. Accepted October 12, 2008. This work was supported by the Korea Research Foundation Grant funded by the Korean Government (MOEHRD) (KRF-2005-041-D00181).

JE8000443